# A semi-grand canonical Monte Carlo simulation model for ion binding to ionizable surfaces: Proton binding of carboxylated latex particles as a case study

Sergio Madurga,[1,a)] Carlos Rey-Castro,[2] Isabel Pastor,[1] Eudald Vilaseca,[1] Calin David,[2] Josep Lluís Garcés,[2] Jaume Puy,[2] and Francesc Mas[1]
[1]*Department of Physical Chemistry and Research Institute of Theoretical and Computational Chemistry (IQTCUB), University of Barcelona (UB), C/ Martí i Franquès, 1, E-08028 Barcelona, Spain*
[2]*Department of Chemistry, University of Lleida (UdL), Av. Rovira Roure, 191, E-25198 Lleida, Spain*

(Received 9 May 2011; accepted 17 October 2011; published online 10 November 2011)

In this paper, we present a computer simulation study of the ion binding process at an ionizable surface using a semi-grand canonical Monte Carlo method that models the surface as a discrete distribution of charged and neutral functional groups in equilibrium with explicit ions modelled in the context of the primitive model. The parameters of the simulation model were tuned and checked by comparison with experimental titrations of carboxylated latex particles in the presence of different ionic strengths of monovalent ions. The titration of these particles was analysed by calculating the degree of dissociation of the latex functional groups vs. *p*H curves at different background salt concentrations. As the charge of the titrated surface changes during the simulation, a procedure to keep the electroneutrality of the system is required. Here, two approaches are used with the choice depending on the ion selected to maintain electroneutrality: counterion or coion procedures. We compare and discuss the difference between the procedures. The simulations also provided a microscopic description of the electrostatic double layer (EDL) structure as a function of *p*H and ionic strength. The results allow us to quantify the effect of the size of the background salt ions and of the surface functional groups on the degree of dissociation. The non-homogeneous structure of the EDL was revealed by plotting the counterion density profiles around charged and neutral surface functional groups. © *2011 American Institute of Physics*. [doi:10.1063/1.3658484]

## I. INTRODUCTION

Much effort has been dedicated to understand the role of electrostatics in soft matter on the theoretical, computational, and experimental fronts.[1] Functionalized latex particles are frequently used as an experimental model of charged particles.[2–8] These particles have acid-base ionizable groups, which are responsible for the surface charge due to their dissociation and subsequent release of counterions in solution. The properties of this kind of materials are strongly influenced by the electrostatic effects that take place at the interface. The presence of charged surface functional groups implies a non-homogeneous distribution of ions around the surface (electric double layer, EDL). In these systems, the structure of the EDL depends on the characteristics of the solution (*p*H and ionic strength), and the counterions (e.g., size and valence).[9]

Many studies have been devoted to characterizing the polyelectrolyte effect in the processes of ions binding to natural complexants. Much of the work is undertaken within the context of mean-field theories, which allow the definition of the so-called surface potential. Once the surface potential is known, the electrostatic contribution to the binding energy and the specific binding can be obtained straightforwardly (see Ref. 10, and references quoted therein).

Apart from the mean-field theories work, considerable research has been addressed to characterizing the distribution of ions around a charged surface, which is often modelled as a continuous distribution of charge (see Ref. 11, and references quoted therein). Several attempts have been made to include the discreteness of the surface charge or to discuss the approximations implicit in the integration of the Poisson equation when computing the potential profile of the EDL around a discretely charged surface. The effect on the counterion density around a discrete macroion charge distribution in spherical colloids was analysed in the context of the primitive model by Messina using molecular dynamics (MD) calculations[12,13] and by Ravindran and Wu by Monte Carlo (MC) simulations.[14] For discretely charged planar surfaces, canonical MC simulations have been performed to study the EDL structure in the presence of different electrolytes[15] and also in the presence of mixtures of electrolytes.[16,17] Recently, Faraudo and Travesset[18] studied the effect of discrete charges at an interface consisting of a phosphatidic acid lipid domain in contact with an ionic solution using explicit water molecules. In order to study the ion-ion correlations and the effect of finite ion size on specific ion binding to polyelectrolyte surfaces, MC simulation methods have been applied in recent years (see Ref. 9, and references quoted therein). Some attempts use semi-grand canonical MC (SGCMC) simulations, combining a grand canonical MC (GCMC) algorithm for the ion binding, and a canonical MC description (CMC)

a)Author to whom correspondence should be addressed. Electronic mail: s.madurga@ub.edu. Fax: +34 934021231.

 

for the rest of the ions in the supporting electrolyte.[19–22] Simulations of linear polyelectrolytes with explicit counterions have been performed by Panagiotopoulos[23] using the reactive CMC method.[24] Jönsson and co-workers have developed a grand canonical titration (GCT) method, similar to the SGCMC method, but using only the grand canonical ensemble within the primitive model to describe the charge process at solid/liquid interfaces in contact with an electrolyte solution at different ionic strengths.[25–27] The effect of the ionic medium is taken into account by fixing the chemical potential of the ions, either near a single charged surface, or between two charged surfaces, to the value obtained under bulk conditions. These chemical potentials were calculated in separated simulations in the canonical ensemble using the Widom insertion technique. This new simulation algorithm has been applied to the simulation of the charged solid/liquid interfaces of calcium silicate hydrate[25,28] and clay particles.[26,29–32] The simulations show good agreement with experimental data. In particular, they show the overcharging process with divalent ions[30] which is a well-known phenomenon that can only be explained by moving beyond typical mean-field theories.[7,8] As in the SGCMC simulations, when a new fixed charge is generated at the surface, a new free counterion is added or a new free coion is removed from the simulation cell to maintain the electroneutrality of the system.[27] They showed differences between the two procedures, and they developed[27] a correction to the method that takes into account the chemical potential of the free added/removed ion. This correction provides concordance between the two methods and it is very close to the uncorrected coion procedure.

Recently, we have developed a SGCMC simulation method in the context of the primitive model to study the acid-base titration process of charged particles with weak-acid surface functional groups.[22] In this method, only the chemical potential of the protons is imposed, as in the standard grand canonical ensemble. Thus, this method differs from the standard GCMC method in its *semi* term because the variation of the surface charge is constrained by the total number of functional groups and the simulation cell is connected with an infinite proton reservoir. In this SGCMC, we apply an iterative procedure to find the appropriate quantity of ions of the inert salt that gives the desired bulk concentration at large distances from the charged surface. In the paper that we published recently,[22] the electroneutrality of the system was maintained by adding or removing a counterion to generate or eliminate a surface charge. Here we also consider the other procedure for maintaining electroneutrality, i.e., the addition or deletion of a coion. It is important to note that these two procedures are not equivalent as pointed out by Labbez and Jönsson[27] because in the calculation of the system free energy the excess chemical potential associated with the free added or removed ions is not taken into account.

The ions of the inert salt are modelled as charged hard spheres, the solvent is treated as a dielectric continuum, and the charged particle is represented as a discretely charged flat surface. In contrast to simple models that consider the charged wall as a surface with a continuous distribution of charge,[11] in these simulations a discrete charge distribution was considered. Hence, the ionized functional groups were modelled as an array of charged sites distributed across the surface. In addition, this model allowed us to analyse the effect of the shape of the functional group by considering different distances between the charged sites and the surface. Also, different ion sizes are considered for the ions of the inert salt, from values representing the bare ionic radius to hydrated radii values. We also analyse the differences between the two procedures for neutralizing a surface charge by the addition of a counterion or the deletion of a coion. The comparison of the results obtained with hydrated and non-hydrated sizes allows us to analyse the effect of ions near the charged surface losing their solvation water molecules. The probability of binding depends on both the *p*H and the intrinsic stability constant. Thus, the use of this SGCMC method allows the functional groups of the surface to be in equilibrium with an electrolyte solution at a fixed *p*H value.

The aim of this paper is to validate our SGCMC simulation model by comparing it to well-described titration experiments on a typical latex particle in the presence of monovalent ions. Our results will also be compared with the description given by mean-field approximations.[33] Latex particles are spherical particles with a radius of hundreds of nm. Thus, a surface complexation model using planar geometry should be adequate to rationalize the polyelectrolytic effect in this kind of system. In addition, MC simulations allow us to analyse ion distributions over non-planar surfaces which is not possible in a simple Poisson Boltzmann (PB) approximation. In future calculations, the surface model obtained will be used in conditions where mean-field approximations do not describe the system correctly, as in the case of divalent or trivalent ionic solutions.

The organization of the paper is as follows: in Sec. II, we summarize the binding process in mean-field theories. Section III is devoted to the SGCMC simulation method. In Sec. IV the results obtained are described and analysed, and the applicability of the simulation procedure is discussed. Comparison with the PB model is also considered. Finally, the main conclusions of this work are summarized in Sec. V.

## II. THEORETICAL BACKGROUND

The interactions of small ions with natural complexants in aqueous media (small ligands, macromolecules, and surfaces) play an important role in the bioavailability and toxicity of these elements.[10,34] All these interactions can be schematized as

$$(-\mathrm{L})^{z-}_{\mathrm{aq/s}} + \mathrm{M}^{n_+}_{\mathrm{aq}} \overset{K^{\mathrm{app}}_{\mathrm{bin}}}{\rightleftharpoons} (-\mathrm{LM})^{n_+ + z-}_{\mathrm{aq/s}}, \qquad (1)$$

where $-$L represents a generic binding site of a surface molecule and $\mathrm{M}^{n_+}_{\mathrm{aq}}$ represents an inorganic ion or a proton. In most cases $-$L does not behave as an ideal (homogeneous) ligand and the value of the apparent binding affinity, $K^{\mathrm{app}}_{\mathrm{bin}}$, is not a constant. Rather, $K^{\mathrm{app}}_{\mathrm{bin}}$ often depends on the metal concentration due to the presence of sites with different chemical functionalities, the presence of mutual interactions between sites, conformational changes in the macromolecule, aggregation processes, etc.[9,35,36] This fact is referred to as

*chemical heterogeneity*. Moreover, both *p*H and ionic strength influence the net charge of the macromolecule/surface and modulate the electrostatic interactions between cations and binding sites. This phenomenon is usually referred to as *polyelectrolytic effect*.[9,10,34]

The acid-base equilibrium of charged surfaces is generally described by the Henderson-Hasselbach equation

$$pK_{\rm dis}^{\rm app} = \log\left(K_{\rm bin}^{\rm app}\right) = p{\rm H} - \log\left(\frac{\alpha}{1-\alpha}\right), \tag{2}$$

where $K_{\rm dis}^{\rm app} = \left(K_{\rm bin}^{\rm app}\right)^{-1}$ is the apparent dissociation constant of the surface and $\alpha$ is the degree of dissociation. Equation (2) can be rewritten in terms of the proton coverage, $\theta$, or the charge density of the surface, $\sigma$, as[10]

$$pK_{\rm dis}^{\rm app} = p{\rm H} + \log\left(\frac{\theta}{1-\theta}\right) = p{\rm H} + \log\left(\frac{\sigma_{\rm max}-\sigma}{\sigma}\right), \tag{3}$$

where $\theta = 1-\alpha = (\sigma_{\rm max}-\sigma)/\sigma_{\rm max}$ and $\sigma_{\rm max}$ is the maximum charge density in the fully deprotonated surface.

In mean-field approximation theories, the free energy of the proton binding process can be separated into two terms: one of electrostatic origin, written as $F\Psi_{\rm S}$ and which gives rise to the electrostatic binding; and a second one of chemical origin, $-RT\ln(K_{\rm c})$, responsible for the specific binding.[10,34] Within the mean-field approximation, $\Psi_{\rm S}$ is the surface potential close to the binding sites with respect to the bulk solution, $F$ is the Faraday constant, $R$ is the ideal gas constant, and $T$ is the temperature.

Then, the apparent binding constant can be factorized as $K_{\rm bin}^{\rm app} = K_{\rm c}\exp(-\tilde{\Psi}_{\rm S})$, where $\tilde{\Psi}_S = \frac{F\Psi_{\rm S}}{RT}$ is the dimensionless surface potential and $K_{\rm c}$ is the average equilibrium function,[10,35] which is related to the specific binding affinity by

$$\begin{aligned}\log(K_{\rm c}) &= -\log(c_{\rm H_S}) + \log\left(\frac{1-\alpha}{\alpha}\right)\\ &= -\log(c_{\rm H_S}) + \log\left(\frac{\sigma_{\rm max}-\sigma}{\sigma}\right),\end{aligned} \tag{4}$$

where $c_{\rm H_S} = c_{\rm H}\exp(-\tilde{\Psi}_{\rm S})$ refers to the volume concentration of protons close to the surface and is related to the bulk concentration by a Boltzmann distribution.

For a homogeneous surface, the average equilibrium function, $K_{\rm c}$, defined in Eq. (4), usually becomes constant and is then referred to as the intrinsic stability constant, $K_0$.

In order to obtain the surface potential, an electrostatic model must be considered, and it can be validated by obtaining a master curve,[10,22,37,38] i.e., all the binding curves ($\sigma$, $\alpha$) vs. *p*H, for different ionic strength, merge when they are plotted in terms of $p{\rm H_S} = -\log(c_{\rm H_S})$ instead of *p*H; this is a master curve.

A classical electrostatic model for charged surfaces is the non-linear Poisson-Boltzmann equation using planar geometry[9] which for symmetric electrolytes gives an explicit relationship between surface charge density and surface potential[39]

$$\sigma = \frac{\sqrt{8\varepsilon IRT}}{z}\sinh\left(\frac{z\tilde{\Psi}_{\rm S}}{2}\right), \tag{5}$$

where $\varepsilon$ is the permittivity of the solution, $I$ is its ionic strength, and $z$ is the charge of the symmetric electrolyte.

It should be noted that for spherical charged particles, the use of a planar geometry is an approximation. To check the validity of this approximation in the context of spherical latex particles of nm scale, a second-order $\sigma - \tilde{\Psi}_{\rm S}$ relationship given by Oshima[39] that takes into account the radius of the particles has been compared with the results obtained with Eq. (5). For symmetrical electrolytes, this expression reads

$$\begin{aligned}\sigma = \frac{\sqrt{8\varepsilon IRT}}{z}\sinh\left(\frac{z\tilde{\Psi}_{\rm S}}{2}\right)\Bigg[1 + \frac{1}{\kappa a}\left(\frac{2}{\cosh^2\left(\frac{z\tilde{\Psi}_{\rm S}}{4}\right)}\right)\\ + \frac{1}{(\kappa a)^2}\left(\frac{8\ln\left[\cosh\left(\frac{z\tilde{\Psi}_{\rm S}}{4}\right)\right]}{\sinh^2\left(\frac{z\tilde{\Psi}_{\rm S}}{2}\right)}\right)\Bigg]^{1/2},\end{aligned} \tag{6}$$

where $\kappa = \sqrt{2IF^2/(\varepsilon RT)}$ is the inverse of the Debye length and $a$ is the radius of the sphere. This expression is in excellent agreement with the exact computational results of Loeb *et al.*[40] with a relative error of less than 1% for $0.5 \le \kappa a < \infty$.[39]

The expressions (5) and (6) have been compared using the habitual experimental conditions found in the literature for latex particles. A range of spherical radii particles of $a \in (50, 155)$ nm, a range of ionic strengths of $I \in (0.01, 0.1)$ M, which yields a value of $\kappa a > 15$, and a range of charge density of $\sigma \in -(0.1, 1.3)$ C m$^{-2}$, were used. In all of these cases, the maximum relative error obtained using the planar geometry expression (5) instead of the second-order approximated spherical expression (6), is less than 2% (results not shown). These results justify the use of planar instead of spherical geometry for latex particles under the experimental conditions given above.

For a homogeneous surface, the binding master curve must follow a Langmuirian binding isotherm in terms of the surface concentration[9,10,22]

$$\theta = (1-\alpha) = \frac{K_0 c_{\rm H}\exp(-\tilde{\Psi}_{\rm S})}{1 + K_0 c_{\rm H}\exp(-\tilde{\Psi}_{\rm S})} = \frac{K_0 c_{\rm H_S}}{1 + K_0 c_{\rm H_S}}, \tag{7}$$

The PB model is a mean-field theory that considers the ions of the electrolyte as point charges and there to be a continuous charge distribution over the surface. Monte Carlo simulations must be performed in order to overcome these limitations, in particular, a charged surface with discrete charges must be considered with a geometry as similar to the molecular structure of the functional groups as possible, as must a size for the ions in solution and the correlations among them.[9,11,15,22,41]

## III. MODEL AND SIMULATION PROCEDURE

The equilibrium properties of the ionic solution in contact with the charged surface (where binding processes occur) were obtained through Monte Carlo computer simulations performed on the SGCMC at a temperature of 25 °C. The solution was modelled as a collection of $N^+$ positive ions and $N^-$ negative ions confined in a rectangular prism of

dimensions $W \times W \times L$. The squared charged wall was situated at $z = 0$. This wall and the uncharged one opposite at $z = L$ were treated as impenetrable with respect to the ion displacements. In contrast, periodic boundary conditions and the minimum image convention[11,15] were employed in the $x$ and $y$ directions. The values for $N^+$ and $N^-$ used were those that yield a concentration profile which at distances far from the charged surface stabilizes around a value that is the desired bulk concentration. Normally, two or three simulations are needed to find the appropriate $N^+$ and $N^-$ values using the counterion or coion procedure, respectively.

Ions were treated as charged hard spheres. Two limiting values of the radius, $a$, were considered: the bare ionic radius and the hydrated ionic radius. The bare ionic radii values were 0.15 nm for $K^+$ and 0.18 nm for $Cl^-$. Whereas, for the hydrated ionic radii, the values were 0.33 nm for $K^+$ and 0.33 nm for $Cl^-$.[15,41] Water solvent molecules were not explicitly considered. Instead, their dielectric constant was introduced in the ion-ion interaction energy expressions. The interaction energy between two ions with charges $Z_i$ and $Z_j$ separated by distance $r$ is

$$\begin{cases} u(\vec{r}) = \frac{Z_i Z_j e^2}{4\pi\varepsilon r} & r \geq d, \\ u(\vec{r}) = \infty & r < d, \end{cases} \tag{8}$$

where $d$ is the sum of the radii of the two particles, $\varepsilon$ is the permittivity of the dielectric continuum, and $e$ is the elementary charge. A modified version of the charged sheet method of Boda and co-workers[15,42,43] was implemented to correct the effects of truncating long-range interactions. For every ion in the solution, this method defines a sheet of infinite dimensions outside the simulation box, parallel to the charged wall and with the same charge as the ion. This is used to compute the long-range Coulomb interactions. The modification treats the movement of ions and the movement of their corresponding charged sheet separately in order to reduce the size dependence of the original method.

The charged wall represents a distribution of ionizable functional groups on a carboxylated latex surface. Its dimensions were kept fixed at $25.6 \times 25.6$ nm$^2$ in all the simulations and the ionizable functional groups were modelled as a surface array of 400 ($20 \times 20$) hard spheres with a finite radius of 0.1 nm which may be neutral or negatively charged. A radius of 0.1 nm was chosen as an approximation of the radius of one of the oxygen atoms of the carboxylate functional group which can be neutral with a hydrogen attached, or negatively charged. According to the array distribution of the surface sites as a square grid, adjacent surface spheres (surface sites) were separated by a distance of 1.28 nm, giving which is the experimental value for the latex particles given in Ref. 33. The surface sphere-ion interaction energy was calculated as in the ion-ion case. The third dimension of the simulation box ($L$) was fixed at 30 nm, imposing a total number on the ions in the solution that ranged from 188 to 6910, depending on the bulk concentration. Three surface models were considered depending on the position of the surface spheres: (i) located at $z = 0$, on the latex surface ($Surf_0$ model), (ii) located at $z = 0.15$ nm ($Surf_{0.15}$ model), and (iii) located at $z = 0.3$ nm ($Surf_{0.3}$ model) from the surface towards the solution

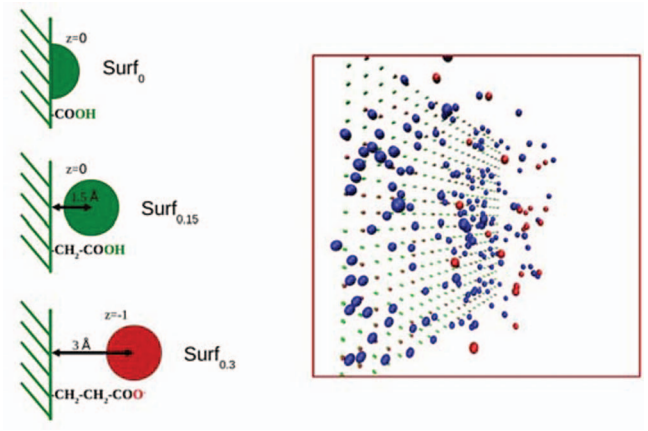


FIG. 1. (Left) Schematic representation of a model surface corresponding to a carboxylated latex particle of large radius. Spheres with a radius of 0.1 nm represent the carboxylated functional groups, either charged or neutral. Their centres are separated 0, 0.15, or 0.3 nm from the surface ($Surf_0$, $Surf_{0.15}$, or $Surf_{0.3}$ models, respectively). (Right) Snapshot of the simulation box with the spheres (charged in red; neutral in green) representing the carboxylated functional groups of the latex surface. Only counterions (blue) and coions (red) closer than a distance of 10 nm to the latex surface are shown.

(Figure 1). The $Surf_0$ model represents a situation in which solution ions are not able to enter the colloid surface. The $Surf_{0.15}$ and $Surf_{0.3}$ models represent cases with carboxylic groups separated, respectively, 0.15 and 0.30 nm from the surface of the latex particle.

When simulating an experiment involving the titration of the polyelectrolyte in the presence of an inert salt at constant ionic strength for a given $p$H, the protons are not explicitly considered in the electrolyte solution. Instead, a set of counterions is introduced in a quantity equal to the number of charged surface spheres so as to maintain the global electroneutrality of the system.[19,20,22]

The SGCMC method[19,20] describes the equilibrium between the surface spheres and the electrolyte solution. According to this model, solution ions can move and surface spheres can change their charge status via protonation (neutralization) or deprotonation (charging). To maintain the electroneutrality of the system, two procedures are possible depending on whether a counterion or a coion is used as the mobile free neutralizing ion. In the first procedure (counterion procedure), every surface charge variation is accompanied by the annihilation or creation of a counterion in the electrolyte solution to maintain the electroneutrality of the system. This implies that the total number of charged particles varies. When a protonation process occurs, a counterion in the solution is selected at random and annihilated. In the deprotonation process, a space position suitable for a counterion insertion is selected at random, and then, the new counterion is introduced in the solution. In the corresponding procedure for a coion (coion procedure), the ion is inserted in the protonation process and it is annihilated in the deprotonation process. In contrast with the previous procedure, the total number of charged particles in the system is now kept constant. A proposed protonation/deprotonation process can only take place after the MC energy test has succeeded. According to Eq. (1), the free energy change, $\Delta F$, for this test, has to be expressed

as

$$\begin{cases} \Delta F = \Delta U_{\text{el}} + k_{\text{B}}T \ln(10)\,(p\text{H} - \log(K_0)) \\ \qquad \text{for protonation process,} \\ \Delta F = \Delta U_{\text{el}} - k_{\text{B}}T \ln(10)\,(p\text{H} - \log(K_0)) \\ \qquad \text{for deprotonation process,} \end{cases} \tag{9}$$

where $\Delta U_{\text{el}}$ is the change in electrostatic energy due to the addition or deletion of charges and $K_0$ is the intrinsic equilibrium protonation constant of the surface sites. The value obtained for $\Delta F$ by SGCMC simulations depends on the procedure chosen to keep the electroneutrality of the system, since in one procedure the total number of charged particles varies and in the other it is kept constant. This implies that for a given $p$H the total number of ions in solution varies in a different way. This effect should be taken into account in the calculation of the total free energy change of the protonation/deprotonation process to obtain the same value of $\Delta F$. It has to be taken into account that the $p$H only enters via Eq. (9) and that $H^+$ and $OH^-$ are not explicitly considered. This is a good approximation when the ionic strength is greater than $[H^+]$ and $[OH^-]$. For each SGCMC simulation 25 000 000 system configurations were generated. The property values were averaged over configurations separated by 1000 particle move steps, with the first 5 000 000 configurations used to equilibrate the system. 3D density profiles were obtained from simulations with 800 000 000 system configurations. A protonation/deprotonation test was performed after every 1000 accepted particle displacements. The probability factor that controls this frequency depends on the simulation conditions and was adjusted automatically during the equilibration period. The simulations were performed using a code developed in C under LINUX operating system on a 76 central processing unit (CPU) cluster.

## IV. RESULTS AND DISCUSSION

In this section, we study the titration profiles of the latex surface using the counterion or the coion procedure. First, we will analyse the results obtained with the counterion procedure. Although this procedure gives non-exact values because the variation of the total number of charged particles is not taken into account in the calculation of $\Delta F$, the iterative process performed to ensure that the concentration profile of the ions in solution tends to the desired value of the bulk ionic strength converges faster. Figure 2 shows the simulation results for the dependence of the degree of dissociation of the functional groups of the latex surface, $\alpha$, on the $p$H of a 0.01 M KCl solution. Three surface models ($\text{Surf}_0$, $\text{Surf}_{0.15}$, and $\text{Surf}_{0.3}$) were considered and the hydrated ionic radii values were used for the counterions (0.33 nm) and coions (0.33 nm). The titration curves were calculated considering two different $\log(K_0/\text{M}^{-1})$ values for the carboxylic functional groups on the latex surface: 4.4, which is obtained from the fitting to experimental data of polycarboxylic acids[10] and 4.9, which is obtained from carboxylated latex particles.[33] The comparison with experimental curves (taken from Figure 1(a) of Ref. 33) shows that when using a charged site-surface separation of 0.15 nm ($\text{Surf}_{0.15}$ model) with a $\log(K_0/\text{M}^{-1})$value of 4.9, the simulations yield the best agreement with the experimental results.

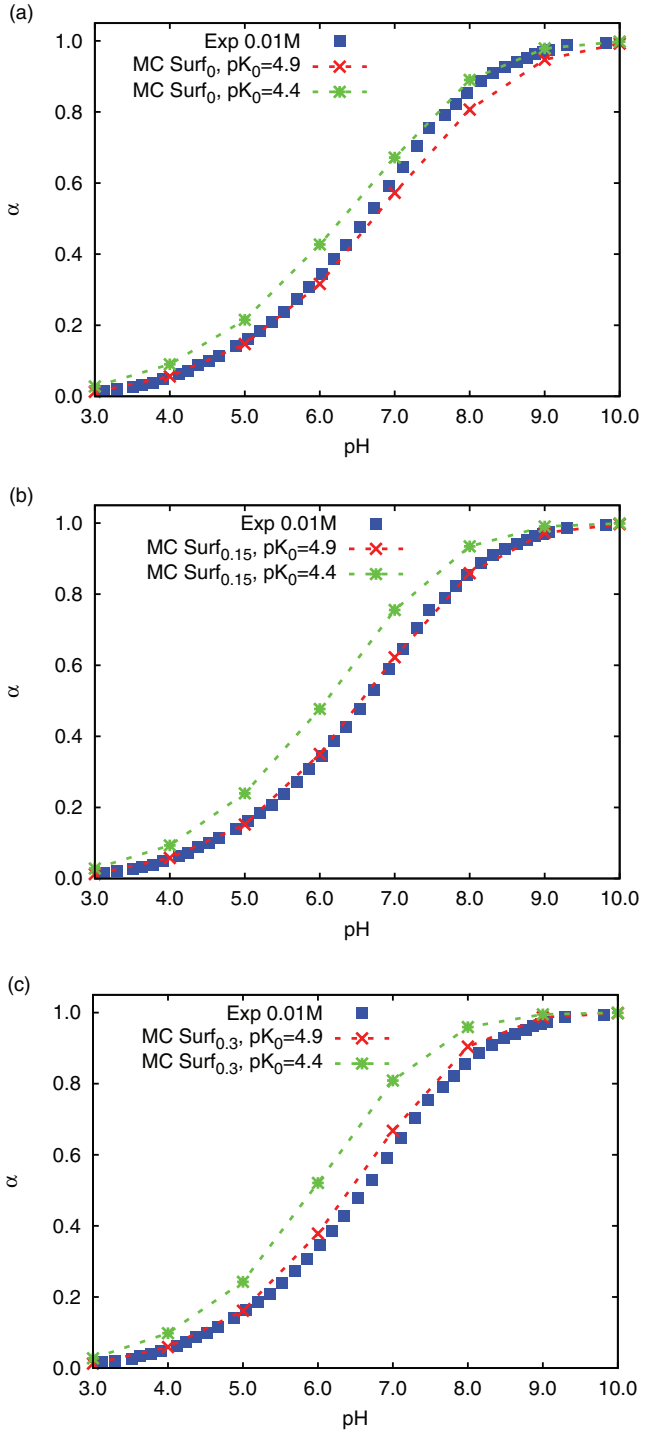


FIG. 2. Comparison between experimental data (from Ref. 33, in filled squares) and SGCMC simulation values (counterion procedure) for the degree of dissociation ($\alpha$) as a function of $p$H for a 0.01 M KCl solution obtained using a $\log(K_0/\text{M}^{-1})$ value of 4.9 (crosses) and 4.4 (asterisks), and the hydrated radii for $K^+$ (0.33 nm) and $Cl^-$ (0.33 nm) ions. The profiles for the (a) $\text{Surf}_0$, (b) $\text{Surf}_{0.15}$, and (c) $\text{Surf}_{0.3}$ surface models are shown.

For all three surface models, the MC curves obtained for a 0.01 M KCl solution with a $\log(K_0/\text{M}^{-1})$ value of 4.9 are more similar to the experimental data than the MC curves obtained with a $\log(K_0/\text{M}^{-1})$ value of 4.4. In order to obtain a

MC $\alpha$ vs. $p$H profile similar to that obtained experimentally, selection of the appropriate $\log(K_0)$ value for the functional groups and selection of the appropriate surface model is an important requirement. It can be seen that differences in $\alpha$ among surface models, for the same $\log(K_0)$ value, are very small at low $p$H values but are important at high $p$H values. To rationalize this behaviour, it is necessary to take account of the destabilizing electrostatic interactions among surface charged sites and the stabilizing electrostatic interactions of surface charges with bulk counterions, this last contribution depends on the surface model. At high $p$H values, higher values of $\alpha$ were obtained for the model whose surface sites were more separated from the surface, because the charged surface sites can be screened more efficiently. That is because they can be surrounded by a greater quantity of counterions which can compensate the site-site electrostatic repulsion and favour an increase in the number of charged surface sites. At lower $p$H values, corresponding to a surface charge proportion of less than 20%, the effect of the surface site separation is very weak, and all three models can fit the experimental data in this region similarly.

The effect of the size of $K^+$ and $Cl^-$ ions on the degree of dissociation at each $p$H was also analysed (Figure 3). For this purpose, SGCMC simulations were repeated for the three surface models but considering the bare ionic radii for the counterions and coions (0.15 nm for $K^+$ and 0.18 nm for $Cl^-$) and taking 4.9 as $\log(K_0/M^{-1})$. As in the simulations with hydrated ionic radii, we found that, at a fixed $p$H, the value of the degree of dissociation increased with the distance of the charged surface sites from the surface plane ($\alpha_{Surf_{0.3}} > \alpha_{Surf_{0.15}} > \alpha_{Surf_0}$). Again, this trend is explained by the greater reduction of the site-site repulsions among the more separated charged sites thanks to being more effectively screened by counterions. However, all three simulation profiles obtained with bare ionic radii overestimate the experimental curve at 0.01 M (Figure 3). Moreover, comparison of the SGCMC simulation curves for hydrated ionic radii (Figure 2) with those for bare ionic radii (Figure 3) shows an important effect of the ion radius on the degree of dissociation. It can be seen that, for a given $p$H, the value of $\alpha$ increases as the radius of the added inert salt decreases. This increase is a consequence of the better screening of the charged surface sites when the counterions are smaller, which causes a greater reduction of the repulsive interactions between these sites. In contrast, when ions with larger radii are present among the surface sites, the screening effect is smaller and the deprotonation (charging) of the sites is favoured less. Comparison of the SGCMC simulations with the experimental results at $I = 0.01$ M indicates that the hydrated radii values in combination with the $Surf_{0.15}$ surface model give the most reliable description of the titration process. It should be taken into account that the results depend on the minimum distance of approach of the mobile ions to the surface sites and not only on the individual ion radius. For this reason, to analyse the effect of mobile ions, the radius of the surface sites was considered fixed in all the simulations at a reasonable radius corresponding to a non-hydrated oxygen of a carboxylate functional group.

Figure 4 shows the titration profiles obtained from SGCMC simulations for 0.1, 0.03, and 0.01 M ionic strengths,

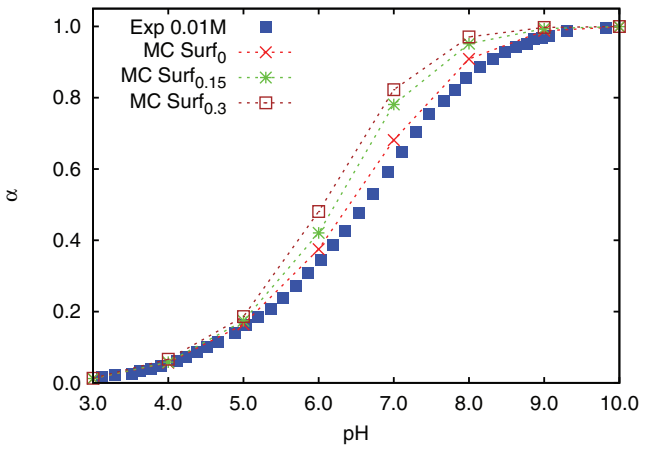


FIG. 3. Comparison between experimental data (filled squares) and SGCMC simulation values (counterion procedure) for the degree of dissociation ($\alpha$) as a function of $p$H in a 0.01 M KCl solution obtained using the bare ionic radii for $K^+$ (0.15 nm) and $Cl^-$ (0.18 nm) ions and considering the (a) $Surf_0$ (crosses) (b) $Surf_{0.15}$ (asterisks), and (c) $Surf_{0.3}$ (open square) surface models.

using $\log(K_0/M^{-1}) = 4.9$ as mentioned above together with the hydrated radii for $K^+$and $Cl^-$. It can be seen that with these values the experimental curves[33] are well reproduced at concentrations of 0.03 M and 0.01 M. Curves obtained using the PB model with the same $\log(K_0)$ and $\sigma_{max}$ values as in these simulations are also shown. Only in the curves for 0.1 M ionic strength, can a small overestimation of $\alpha$ values at high $p$H values be seen for both the PB model and the SGCMC simulations.

If we follow the same procedure in order to optimize the simulation parameters using the alternative method for neutralizing a surface charge consisting of the deletion of a coion, we obtain the titration profiles shown in Figure 5. We found that the $Surf_{0.15}$ surface model in combination with the experimental value of 4.4 for $\log(K_0/M^{-1})$[10] and using the hydrated radii for the ions (0.33 nm for $K^+$ and 0.33 nm for $Cl^-$) were

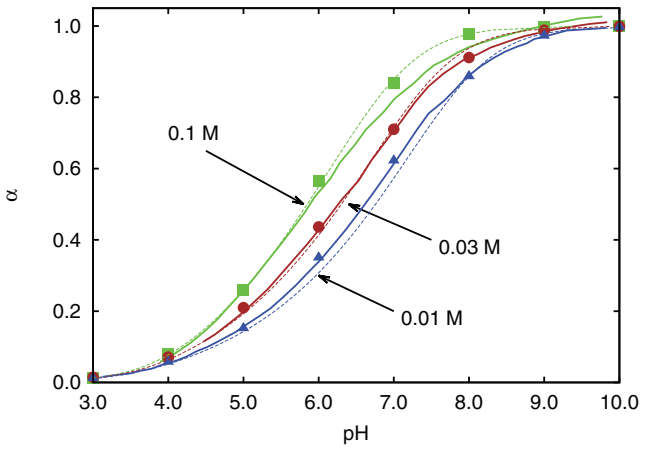


FIG. 4. Comparison between experimental data (from Ref. 33) (continuous lines) and SGCMC simulation values (counterion procedure) for the degree of dissociation ($\alpha$) (symbols) as a function of $p$H in 0.1 M (green line and square), 0.03 M (brown line and circle), and 0.01 M (blue line and triangle) KCl solution obtained using $\log(K_0/M^{-1}) = 4.9$ and the hydrated radii for $K^+$ and $Cl^-$ ions with the $Surf_{0.15}$ surface model. Profiles obtained with the PB model are also indicated (dashed lines).

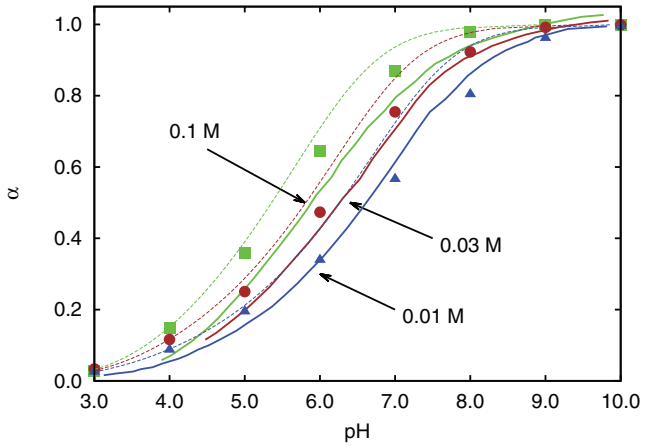


FIG. 5. Comparison between experimental data (from Ref. 33) (continuous lines) and SGCMC simulation values (coion procedure) for the degree of dissociation ($\alpha$) (symbols) as a function of $p$H in 0.1 M (green line and square), 0.03 M (brown line and circle), and 0.01 M (blue line and triangle) KCl solution obtained using $\log(K_0/\mathrm{M}^{-1}) = 4.4$ and the hydrated radii for $K^+$ and $Cl^-$ ions with the $\mathrm{Surf}_{0.15}$ surface model. Profiles obtained with the PB model are also indicated (dashed lines).

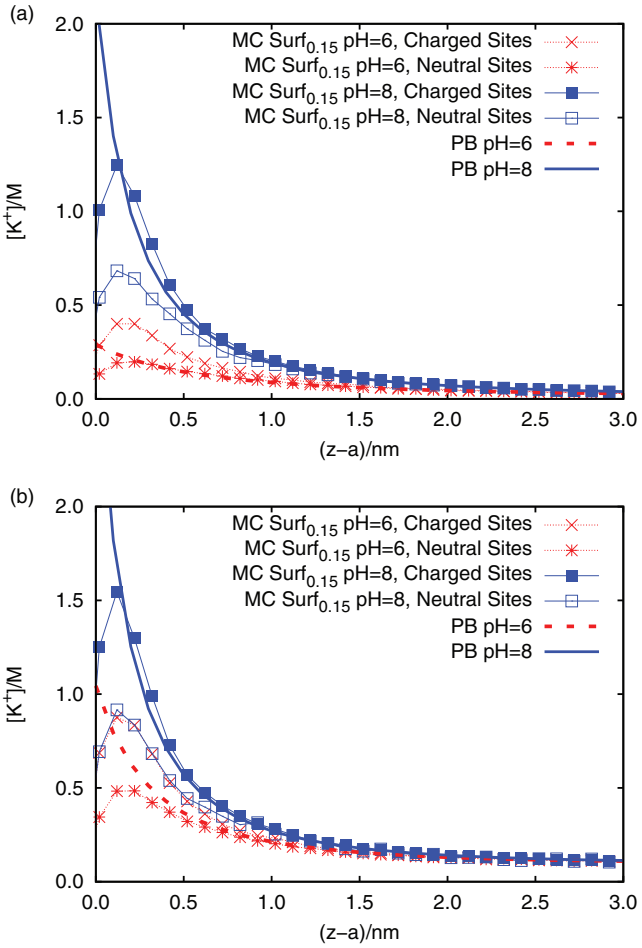


FIG. 6. Counterion densities for charged and neutral sites in a 0.01 M (a) and 0.1 M (b) KCl solution as a function of the distance from the surface at $p\mathrm{H} = 6$ and 8 using the counterion procedure. The $a$ parameter stands for the counterion radius ($a = 0.33$ nm for simulation profiles and $a = 0$ nm for PB profiles).

good enough to reproduce the tendency of the experimental titration curves. This $\log(K_0)$ value was obtained from titration experiments of polyacrylic acid. It can be seen that, as in the counterion procedure, the simulation curve for 0.01 M ionic strength is the closest to the experimental values. For higher ionic strengths, simulation results show a small overestimation. However, it should be noted that the curves obtained using the PB model with the value of 4.4 for $\log(K_0/\mathrm{M}^{-1})$ were now very far from the experimental values.

Although in our SGCMC method, we perform an iterative procedure which changes the number of ions in solution to ensure that in the bulk concentration profile of ions achieves the value for the ionic strength that we impose, the SGCMC simulations give different results depending on the procedure used to keep the electroneutrality of the system. The difference obtained between the procedures (results not shown) arise from the fact that we do not take into account the correction for the change in the total number of ionic particles during the simulation. Moreover, it seems more plausible that the coion procedure gives more accurate results than the counterion procedure, because the total number of charged particles is kept constant during the protonation/deprotonation processes. This is in accordance with the correction made by Labbez and Jönsson to their GCT method,[27] where the excess chemical potential associated with the inserted or deleted ions is considered in the calculation of $\Delta F$. Thus, from the values obtained in the SGCMC simulations, the value of 4.4 for $\log(K_0/\mathrm{M}^{-1})$ obtained with the coion procedure is more reasonable than the value of 4.9 obtained with the counterion procedure. It is, however, worth pointing out that the optimization of the simulation parameters using these two procedures yields the same parameters except for a difference of $\log(K_0)$, with the procedure of insertion/deletion of a coion giving a greater discrepancy with the PB results.

Additionally, the SGCMC simulations provide a description of the electrolyte ion distribution at different distances from the surface. As the density distribution of counterions around a surface site can be different depending on whether the site is neutral or negatively charged, the density distribution around a neutral site and around a charged site were computed separately. Two types of density profiles were considered: a linear ion distribution along the $z$ coordinate and a bidimensional distribution across the $x$, $y$ plane. To obtain the $z$ density distributions, the space of the system was divided into 400 rectangular cuboids ($1.28 \times 1.28 \times 30$ nm$^3$) each one centred on a surface site. For each MC configuration analysed the counterion distribution along the $z$ direction was computed for each cuboid, and the values obtained for neutral and charged sites were averaged separately. The averaging fact that an ionization state (charged or neutral) of a given site may change from one MC configuration to another was taken into account. Figure 6 shows the averaged counterion density profiles as a function of the distance to a charged surface site and to a neutral surface site, as obtained for the cases with $p\mathrm{H} = 6$ and $p\mathrm{H} = 8$, and for 0.01 M and 0.1 M KCl ionic strengths. The existence of counterion layering near the surface (up to 0.5 nm) can be observed for both the concentrations. This local accumulation of counterions is more important at higher $p$H values due to the higher degree of

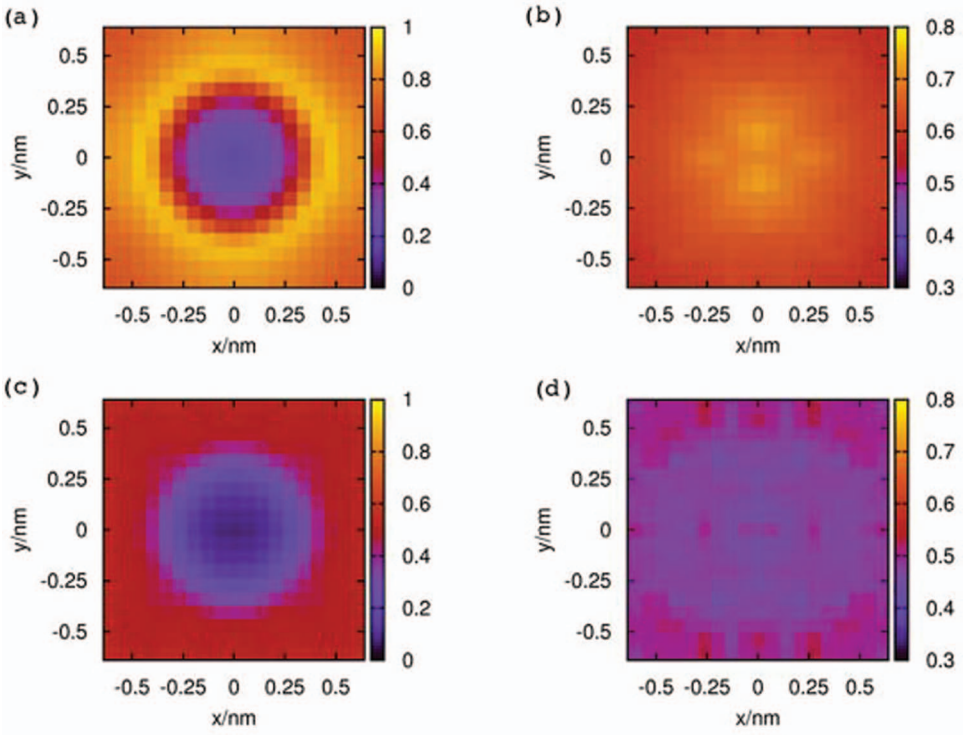


FIG. 7. Bidimensional distribution of $K^+$ ions obtained from a SGCMC simulation (counterion procedure) of a 0.1M KCl solution at *p*H=8 with the $Surf_{0.15}$ surface model for a section (a) between $z = a$ and $z = 2a$ around a charged site, (b) between $z = 2a$ and $z = 3a$ around a charged site, (c) between $z = a$ and $z = 2a$ around a neutral site, and (d) between $z = 2a$ and $z = 3a$ around a neutral site. $a$ is the radius of the hydrated $K^+$ ion.

ionization of the surface, which implies that a higher counterion density is needed to compensate the polyelectrolyte surface charge. In Figure 6, it can also be seen that, as expected, there are more counterions located around the charged surface sites than around the neutral sites. More specifically, the concentration of counterions around charged sites is about twice that around neutral sites for both concentrations and both *p*H values. It should be noted that due to the roughness of the $Surf_{0.15}$ surface model, counterions in contact with the surface plane are located at $z - a = 0$, and those in contact with a surface functional group (sphere) are located at an interval of $z - a$ that ranges from 0 to 0.25 nm. In all the cases, the maximum of the counterion density profiles is situated at this interval. The counterion distribution was also computed using the PB model, taking into account that $a = 0$. The comparison of SGCMC with PB profiles shows that, for all conditions, the PB approximation yields a greater counterion density at the distance of maximum approach to the surface, as is expected for a mean-field theory. However, at larger distances ($z - a > 0.1$ nm), PB profiles show a marked decrease and fall between the SGCMC profiles corresponding to charged and neutral sites.

To analyse the counterion ($K^+$) distribution around the surface sites in the $x$ and $y$ directions, which are parallel to the surface, the set of rectangular cuboids centred on the surface sites was also used. For each cuboid, the average counterion concentration in a small $z$ interval around each $x$, $y$ position was counted. The bidimensional density maps around charged and neutral sites were computed separately. It is worth mentioning that when the surface is modelled as a continuous charged surface and the counterion density is calculated with the PB model, this density is constant at each $z$ distance. In contrast, SGCMC simulations yield great fluctuations of the counterion density in the $x$ and $y$ directions at short distances from the surface (from $z = a$ to $z = 2a$) for both charged (Figure 7(a)) and neutral surface sites (Figure 7(c)). In the case of a charged site, the density goes from 0 M at the centre of the map to a maximum value about 1 M at a distance of 0.44 nm from the centre (Figure 7(a)). For a neutral site, the density goes from 0 M at the centre to a maximum value of about 0.6 M at the corners of the density map (Figure 7(c)). In both cases, there is no $K^+$ density at the central position of the map because of the volume exclusion among counterions and surface sites. At larger distances from the surface, in the region from $z = 2a$ to $z = 3a$, the $x$, $y$ counterion density around the charged surface sites (Figure 7(b)) and the neutral ones (Figure 7(d)) show smaller fluctuations. As expected, greater local concentrations were obtained around charged sites (from 0.6 M to 0.7 M) than around neutral sites (from 0.4 M to 0.5 M). The bidimensional profiles are also different. For the charged sites the maximum density is located at the centre of the map (at this $z$ distance there is no excluded volume effect) while for the neutral sites the maxima are situated at the corners of the map.

From the counterion density analysis with respect to the surface distance (Figure 6) and with respect to the directions parallel to the surface (Figure 7), we observe that PB results and the results from SGCMC simulations with the $Surf_{0.15}$ model are qualitatively and quantitatively different. However, the profiles of the degree of dissociation vs. *p*H obtained by

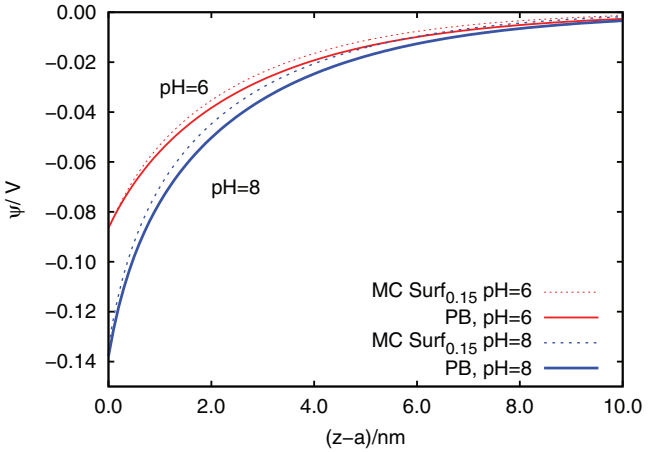


FIG. 8. Electrostatic potential as a function of the distance to the surface for a 0.01 M salt solution at $p$H = 6 (in red) and $p$H = 8 (in blue) obtained from SGCMC simulations (counterion procedure) with the $\text{Surf}_{0.15}$ surface model (continuous line) and from the PB model (dashed line). The $a$ parameter stands for the hydrated radius of $K^+$ ion ($a$ = 0.33 nm for simulation profiles and $a$ = 0 nm for PB results.

the two methods are very similar. In order to understand the reason for this behaviour, we compared the values of the surface potential and the electrostatic potential as a function of the surface distance. In the mean-field PB model, the surface potential can be calculated by means of Eq. (5) for a particular value of surface charge density. For SGCMC simulations, we can obtain an estimation of the surface potential along the $z$ coordinate (normal to the charged surface) calculating the average value of the electrostatic potential at each distance by using[15,22]

$$\Psi(z) = \frac{1}{N_{z_{\max}}} \sum_{i=1}^{N_{z_{\max}}} \left\{ \frac{1}{N_{\text{conf}}} \sum_{j=1}^{N_{\text{conf}}} \frac{e}{\varepsilon W^2} \times \left( \sum_{k=1}^{N_{\text{ions}}} (z - z_k) Z_k \right); z_k \le z_{\max,j} \right\}, \quad (10)$$

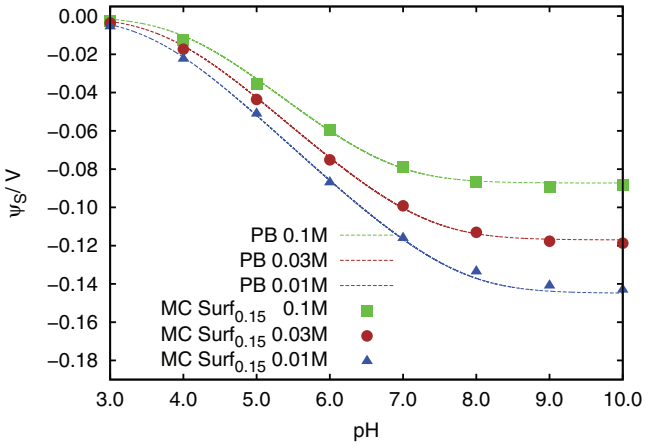


FIG. 9. Surface potential as a function of the $p$H for a 0.1 M (squares), 0.03 M (circles), and 0.01 M (triangles) KCl concentration obtained from SGCMC simulations (counterion procedure) with the $\text{Surf}_{0.15}$ surface model. The PB results are also indicated (dashed lines) for comparison purposes.

where $N_{\text{conf}}$ is the total number of MC configurations used, $N_{\text{ions}}$ is the number of solution ions of the system, and $N_{z_{\max}}$ is the number of $z_{\max}$ distances employed, from which it is reasonable to suppose bulk conditions. Equation (10) gives the profile of the electrostatic potential along the $z$ coordinate. The profiles corresponding to eight different values of $z_{\max}$ from 13 nm to 20 nm from the surface were averaged. The surface potential is the electrostatic potential value at the distance of closest approach of the hydrated $K^+$ ions to the surface, i.e., $\Psi_S = \Psi(z = a)$.

According to Figure 7, the local concentration of ions is not constant in the $x$ and $y$ directions. Thus, since in this calculation the dependence on $x$ and $y$ is ignored, the electrostatic potential obtained from Eq. (10) can be seen as an approximate mean electrostatic potential. Figure 8 shows that PB model and the SGCMC simulations yield similar profiles for the electrostatic potential as a function of the distance to the surface. The greatest differences are observed between 2 and 4 nm. However, very similar values at both $p$H values are obtained at the distance of closest counterion approach. Thus, the mean-field model and SGCMC simulations give similar surface potential values. Figure 9 shows the surface potential vs. $p$H curves obtained from PB model and the SGCMC simulations with the $\text{Surf}_{0.15}$ surface model for KCl concentrations of 0.1 M, 0.03 M, and 0.01 M. The profiles obtained from both the procedures coincide to a high degree.

## V. CONCLUSIONS

This work presents a SGCMC simulation model which is used to describe the process of proton binding to an ionizable surface in contact with an electrolyte solution. The surface is modelled as a plane, the ionizable surface groups as hard spheres with a finite radius of 0.1 nm situated on or separated from the surface plane, and the primitive model is used for the solvent. With this simulation model we aimed to reproduce experimental titrations of functionalized carboxylated latex particles with a maximum charge density value of $\sigma_{\max} = -0.098$ C m$^{-2}$. The simulation model has been validated by comparing the results it yields with experimental titration curves of carboxylated latex particles dispersed in 1:1 electrolyte solutions, with two different procedures simulated to neutralize the charge of the system.

Model parameters such as the separation of the ionizable surface sites from the surface plane, the $\log(K_0)$ value, and the radii of the ions in solution were modified in order to find the values that would best fit with the experimental results. The $\text{Surf}_{0.15}$ surface model in combination with the values of 4.9 (for the counterion procedure) or 4.4 (for the coion procedure) for $\log(K_0/\text{M}^{-1})$ and the hydrated radii for the ions (0.33 nm for $K^+$ and 0.33 nm for $Cl^-$) were found to reproduce the experimental titration curves accurately. However, it seems that the value of 4.4 for $\log(K_0/\text{M}^{-1})$ is the better estimation as the SGCMC simulations performed with the coion procedure seem to be more accurate. This is in accordance with the results reported by Labbez and Jönsson for their GCT method.[27] Selection of the appropriate surface model is important to reproduce the experimental titration curves at high $p$H values, but not so important at low $p$H values.

For the systems studied (1:1 background salt, and relatively low surface charge densities) the SGCMC simulations give a degree of accuracy in the description of the experimental titration data similar to the mean-field PB model. Coincidences in the degree of dissociation vs. *p*H curves are interpreted as a consequence of the two models yielding similar average surface potential values. However, explicit consideration of the surface-site and ion-ion correlation allows the SGCMC simulation model to describe the fluctuations of the counterion distribution near the surface. These fluctuations cannot be described by the PB model. In particular, the simulation results show that the concentration of counterions around the charged sites is double that around the neutral sites. However, it should be taken into account that the PB model for low surface charge density and the monovalent inert salts is powerful enough when we are interested in the dependence of the degree of ionization instead of the counterion density. Nevertheless, the log ($K_0$) values obtained fitting the PB model to the experimental data could be different from those obtained from simulations.

Application of this SGCMC simulation model to describe the binding process to ionizable surfaces in contact with 1:2 and 1:3 electrolyte solutions and also 1:1 in combination with surfaces having high surface charge density values is in progress. In comparison to the mean-field approximations this model will allow us to obtain a more detailed insight on the binding phenomena.

## ACKNOWLEDGMENTS

The authors gratefully acknowledge support for this research from the Spanish Ministry of Science and Technology (Project Nos. UNBA05-33-001 and CTM2009-14612) and from the *Generalitat de Catalunya* (Grant Nos. 2009SGR465 and XRQTCQ). I.P. thanks the Juan de la Cierva programme of the Spanish Ministry of Science for a fellowship.

[1] R. Messina, J. Phys. Condens. Matter **21**, 113102 (2009).
[2] I. Ermolina and H. Morgan, J. Colloid Interface Sci. **285**, 419 (2005).
[3] I. Popa, G. Gillies, G. Papastavrou, and M. Borkovec, J. Phys. Chem. B **114**, 3179 (2010).
[4] J. Hierrezuelo, A. Vaccaro, and M. Borkovec, J. Colloid Interface Sci. **347**, 202 (2010).
[5] P. Ihalainen, K. Backfolk, P. Sirvi, and J. Peltoneny, Colloids Surf., A **354**, 320 (2010).
[6] H. C. Schumacher, M. Alves, C. A. P. Leite, J. P. Santos, E. T. Neto, M. M. Murakami, F. Galembeck, and M. do Amaral, J. Colloid Interface Sci. **305**, 256 (2007).
[7] M. Quesada-Pérez, E. González-Tovar, A. Martín-Molina, M. Lozada-Cassou, and R. Hidalgo-Álvarez, Colloids Surf., A **267**, 24 (2005).
[8] A. Martín-Molina, M. Quesada-Pérez, F. Galisteo-González, and R. Hidalgo-Álvarez, J. Phys. Condens. Matter **15**, S3475 (2003).
[9] M. Borkovec, B. Jönsson, and G. J. M. Koper, in *Surface and Colloid Science*, edited by E. Matijevic (Kluwer Academic, New York, 2001), Vol. 16, Chap. 2.
[10] E. Companys, J. L. Garcés, J. Salvador, J. Galceran, J. Puy, and F. Mas, Colloids Surf.,A **306**, 2 (2007).
[11] M. Quesada-Pérez, E. González-Tovar, A. Martín-Molina, M. Lozada-Casou, and R. Hidalgo-Álvarez, ChemPhysChem **4**, 234 (2003).
[12] R. Messina, C. Holm, and K. Kremer, Eur. Phys. J. E **4**, 363 (2001).
[13] R. Messina, Physica A **308**, 59 (2002).
[14] S. Ravindran and J. Wu, Langmuir **20**, 7333 (2004).
[15] S. Madurga, A. Martín-Molina, E. Vilaseca, F. Mas, and M. Quesada-Pérez, J. Chem. Phys. **126**, 234703 (2007).
[16] P. Taboada-Serrano, S. Yiacoumi, and C. Tsouris, J. Chem. Phys. **123**, 1 (2005).
[17] Z.-Y. Wang and Y.-Q. Ma, J. Chem. Phys. **131**, 244715 (2009).
[18] J. Faraudo and A. Travesset, J. Phys. Chem. C **111**, 987 (2007).
[19] T. Nishio, Biophys. Chem. **49**, 201 (1994).
[20] T. Nishio, Biophys. Chem. **57**, 261 (1996).
[21] I. André, T. Kesvatera, B. Jönsson, K. S. Åkerfeldt, and S. Linse, Biophys. J. **87**, 1929 (2004).
[22] S. Madurga, J. L. Garcés, E. Companys, C. Rey-Castro, J. Salvador, J. Galceran, E. Vilaseca, J. Puy, and F. Mas, Theor. Chem. Acc. **123**, 127 (2009).
[23] A. Z. Panagiotopoulos, J. Phys. Condens. Matter **21**, 424113 (2009).
[24] J. K. Johnson, A. Z. Panagiotopoulos, and K. E. Gubbins, Mol. Phys. **81**, 717 (1994).
[25] B. Jönsson, A. Nonat, C. Labbez, B. Cabane, and H. Wennerström, Langmuir **21**, 9211 (2005).
[26] C. Labbez, B. Jönsson, I. Pochard, A. Nonat, and B. Cabane, J. Phys. Chem. B **110**, 9219 (2006)
[27] C. Labbez and B. Jönsson, Lect. Notes Comput. Sci. **4699**, 66 (2007).
[28] C. Labbez, B. Jönsson, M. Skarba, and M. Borkovec, Langmuir **25**, 7209 (2009).
[29] M. Delhorme, C. Labbez, C. Caillet, and F. Thomas, Langmuir **26**, 9240 (2010).
[30] C. Labbez, A. Nonat, I. Pochard, and B. Jönsson, J. Colloid Interface Sci. **309**, 303 (2007).
[31] C. Labbez, I. Pochard, B. Jönsson, and A. Nonat, Cement Concrete Res. **41**, 161 (2011).
[32] M. Medala, C. Labbez, I. Pochard, and A. Nonat, J. Colloid Interface Sci. **354**, 765 (2011).
[33] S. H. Behrens, D. I. Christl, R. Emmerzael, P. Schurtenberg, and M. Borkovec, Langmuir **16**, 2566 (2000).
[34] J. Buffle, *Complexation Reactions in Aquatic Systems: An Analytical Approach* (Ellis Horwood Ltd, Chichester, 1998).
[35] J. L. Garcés, F. Mas, J. Puy, J. Galceran, and J. Salvador, J. Chem. Soc., Faraday Trans. **94**, 2783 (1998).
[36] J. L. Garcés, F. Mas, J. Cecília, E. Companys, J. Galceran, J. Salvador, and J. Puy, Phys. Chem. Chem. Phys. **4**, 3764 (2002).
[37] J. C. M. Wit, W. H. Riemsdijk, and L. K. Koopal, Environ. Sci. Technol. **27**, 2005 (1993).
[38] D. G. Kinniburgh, W. H. Riemsdijk, L. K. Koopal, M. Borkovec, M. F. Benedetti, and M. J. Avena, Colloids Surf., A **151**, 147 (1999).
[39] *Electrical Phenomena at Interfaces. Fundamentals, Measurements and Applications*, edited by H. Ohshima and K. Furusawa (Marcel Dekker, New York, 1998), Chap. 1.
[40] A. L. Loeb, J. T. G. Overbeek, and P. H. Wiersema, *The Electrical Double Layer, Around a Spherical Colloid Particle* (MIT Press, Cambridge, MA, 1961).
[41] M. Quesada-Pérez, A. Martín-Molina, and R. Hidalgo-Álvarez, J. Chem. Phys. **121**, 8618 (2004).
[42] D. Boda, K. Y. Chan, and D. Henderson, J. Chem. Phys. **109**, 7362 (1998).
[43] D. Boda, W. R. Fawcett, D. Henderson, and S. Sokolowski, J. Chem. Phys. **116**, 7170 (2002).